Soil and Tillage Research 196: 104461 (2020)

Effects of interrill erosion on the distribution of soil organic and inorganic carbon in different sized particles of Mediterranean Calcisols

***Laura Quijano [a], Nikolaus J. Kuhn [b], Ana Navas [c]**

[a] Georges Lemaître Centre for Earth and Climate Research, Université Catholique de Louvain, 1348 Louvain-la-Neuve, Belgium

*E-mail address of corresponding author: laura.quijano@uclouvain.be

[b] Department of Environmental Sciences, University of Basel, Switzerland

E-mail address: nikolaus.kuhn@unibas.ch

[c] Estación Experimental de Aula Dei, Consejo Superior de Investigaciones Científicas (EEAD-CSIC), 1005 Avda. Montañana, Zaragoza, Spain

E-mail address: anavas@eead.csic.es

Abstract

In this study, the potential effect of the selective transport and deposition by interrill erosion on the spatial distribution of eroded soil and associated soil organic (SOC) and inorganic carbon (SIC) in carbonate-rich soils was investigated in Mediterranean cultivated Calcisols. Particular attention was paid to the role of calcium carbonate in the stabilization of SOC and its impact on soil structure and the settling behavior of soil particles in suspension. The settling velocity is a key variable in controlling the transport and fate of eroded sediment and sediment-associated carbon, which accounts for soil particle / aggregate size and density. The objectives were to analyze the settling behavior of cultivated soils at two contrasting slope positions, representative of erosion and deposition sites, in an interrill area and compare with those of uncultivated and undisturbed soils (not affected by deposition or erosion processes). Besides we examined the distribution of SOC and SIC associated with different particle size classes. Soils were fractionated into five size classes (> 250, 125–250, 63–125, 32–63 and ≤32 μm) using a settling tube procedure and carbon contents (SOC and SIC, %) were measured at each settling size classes. The results indicated that the particle size selectivity of interrill erosion affects the distribution of soil particles and associated SOC and SIC spatial variability. As a result of erosion processes, cultivated soil at the upper part of the slope was enriched in finer fractions compared to the lower part where mainly coarse particles were deposited and the finer material was transported and washed out. Cultivation leads to a depletion of SOC and of the >250 μm fraction in comparison with uncultivated and undisturbed soil, where the SOC content was two times higher than in cultivated soil. Lighter and smaller settling size classes (≤63 μm) had the highest SOC content in uncultivated and cultivated downslope soils. This is contrary to what occurs with SIC that acts as a cementing agent and promotes

aggregation formation affecting soil structure. Therefore, sand-sized and siltsized carbonates were accumulated in coarser size fractions in these soils, mainly in downslope positions. This study provides a first insight into the role of selective processes by interrill erosion and their impact on soil organic/inorganic carbon distribution affected by different particle selective transport process, soil aggregate size distribution and associated carbon in Mediterranean agroecosystems.
Keywords: soil erosion; C settling size class; Soil organic and inorganic carbon; Selective transport pattern; Mediterranean area**.**

1. Introduction

Erosion is considered one of the major threats to soils resulting in loss of soil quality and increase soil degradation (Ballabio et al., 2017; Panagos et al., 2016; Navas et al., 2014). It is estimated that 75 Pg of topsoil is redistributed by erosion annually from arable lands worldwide (Borrelli et al., 2017; Berhe et al., 2007; Pimentel et al., 1995), including karstic landscapes (Navas et al., 2013), and affecting the physical and chemical mechanisms that stabilize carbon in soils (i.e. the input and residence time of carbon in soils) and influencing the soil carbon budget (Lal, 2005). Interrill erosion-induced carbon changes and the potential effect of the spatial distribution of eroded soil and associated soil carbon is still not fully understood due to a lack in process understanding of the interplay between soil erosion/transport/deposition and soil carbon mobilization (Bremenfeld et al., 2013; Wang et al., 2013; Kuhn et al., 2012a, b). During soil detachment, soil aggregates are disrupted exposing the physically protected organic carbon increasing the decomposition and mineralization of soil organic carbon (SOC) (Six et al., 2000). Soil particle detachment and transportation in interrill areas is driven by several factors such as rainfall characteristics, slope and soil properties (Issa et al.,

2006). Raindrops detach soil aggregates and primary particles from the soil (Angulo-Martínez et al., 2012; Beguería et al., 2015) and when runoff begins the increase of the turbulence within the flow also intensifies the transport capacity of interrill erosion (Warrington et al., 2009; Meyer et al., 1975). Kuhn and Armstrong (2012) reported that under higher values of rainfall intensity and kinetic energy, erosion may be less selective, decreasing the capacity for faster soil aggregate breakdown and therefore the generation of erodible material. In contrast, under lower intensity rainfall, the size-selectivity of eroded material can be high and aggregate breakdown is limited so that many aggregates are too large for entrainment, and only small and light particles will be mobilized (Kuhn and Armstrong, 2012). A better understanding of the relationships among soil detachment, transport, and deposition on interrill areas will be helpful to interpret experimental data and developing process-based interrill erosion models. The potential of coupled distributed models to track the dynamics of eroded organic material, which depend on a multitude of factors (Berhe et al., 2012), has been widely recognized (Papanicolaou et al., 2015).

The impact of water erosion on cultivated lands is one of the major threats to soil fertility, such as in the Mediterranean mountain region (Lizaga et al., 2018; Barreiro-Lostres et al., 2017; Navas et al., 2008; Lasanta et al., 2006). Land use conversion to cropland associated with a long history of human activity, had important effect on the intensity of soil erosion (Gaspar et al., 2019, 2013; Lizaga et al., 2017) and on the storage and stability of carbon in soils (Quijano et al., 2017, 2016a). In addition, many studies have demonstrated that intensive tillage deteriorates soil structure and enhances soil erosion, thus increasing the rate of carbon mineralization and the loss of SOC (Zheng et al., 2018; Navas et al., 2017; Álvaro-Fuentes et al., 2009; Razafimbelo et al., 2008). The fate of eroded soil particles is strongly related to the transport distance

which is, in-turn, associated with their settling velocities (Hu and Kuhn, 2016). The settling velocity is dependent on a range of variables, including particle size, density and shape, the concentration and the viscosity of water. However, the dominant control can be assumed to be particle size, which in turn is dependent on the particle composition and the source of sediment produced by soil erosion (Loch, 2001; Mantovanelli and Ridd, 2006; Xiao et al., 2015). Soil aggregation potentially increases the settling velocities of soil particles, and consequently reduces their transport distances after erosion (Hu et al., 2013b).

Particle size distribution of eroded sediments related to their settling velocities is required to accurately predict where soil particles and therefore SOC will be deposited (Warrington et al., 2009). Despite the importance of this topic concerning the relationship between soil redistribution and SOC dynamics further work is needed to quantify SOC distribution across soil fractions (Berhe et al., 2014; Van Oost et al., 2007). Soil texture and other site–specific soil characteristics (vegetation type, soil management, topographic position and parent material) play a crucial role in the stabilization of SOC especially in semiarid regions where calcareous soils are abundant. Calcareous soils have 5% content or more inorganic carbon or carbonate calcium equivalent (Asgari Hafshejani and Jafari, 2017). In many semi-arid soils from Mediterranean regions, the presence of primary and/or secondary carbonates is frequent (Fernández-Ugalde et al., 2011). The precipitation of secondary carbonates in these soils can enhance soil aggregation (Martí-Roura et al., 2019) but little is known about the role of carbonates in organic carbon stabilization by stabilizing soil organic matter (SOM) and binding SOM by calcium (Virto et al., 2011) and its influence on soil structure (Zamanian et al., 2016). Furthermore, the distribution of SIC in different soil particle sizes and the quantification of SIC content are often ignored in research on soil

carbon dynamics (Dong et al., 2017; Wu et al., 2009). Therefore in this study, calcareous soils under xeric moisture conditions in the Mediterranean region have been considered to deal with the effects of the selectivity by interrill erosion on soil particle size distribution, and of the associated SOC and SIC along two contrasting slope positions of a cultivated field draining towards an ephemeral incised stream. Soil carbon changes may be significantly different in erosion-dominated (i.e., upslope) areas of a hillslope versus deposition-dominated (i.e., downslope) areas, with significant effects on net gains or losses in the SOC stored in these zones (Van Oost et al., 2006; Wang et al., 2015). We hypothesized that the settling behavior of soil aggregates differs from soils under different slope positions because cultivation and soil physical downslope movement have implications in the spatial patterns of soil particles and of the associated SOC and SIC (Quijano et al., 2016b). The specific objectives of this study were to: i) evaluate the effect of downslope transfer of soil particles and aggregates by runoff on the grain-size distribution ii) compare the settling velocity distribution of sediment generated on cultivated soils affected by interrill erosion to those of non-cultivated soils and under stable conditions, and iii) quantify the SOC and SIC mass contents in different size fractions to infer the impact of lateral movement of soil carbon by interrill erosion. Improving the knowledge of soil erosion and its impact on soil carbon requires a better understanding of the behavior of eroded soil during transport and deposition across landscapes.

2. Materials and methods

2.1 Study area

The study area is a hydrological unit (3846m2) within a cultivated field in the central part of the Ebro Basin in the northeast of Spain (42°25′37″N; 1°13′12″W) (Fig.1a). The

climate is continental Mediterranean. The mean annual temperature is 13.4 °C and the mean annual rainfall is about 500mm (recorded since 1929 at the Yesa reservoir; AEMET) (Lizaga et al., 2019). The field, that is located at the lowest part of a cultivated slope with direct connectivity to an ephemeral stream, was chosen because it is representative of Mediterranean mountain agroecosystems. The field is a rain-fed crop field where winter cereals (Triticum aestivum and Hordeum vulgare L.) have been cultivated for the last 150 years. A digital elevation model (DEM) with high spatial resolution (2.5 m) was created to characterize the land surface in detail at field scale (Fig. 1a) (Quijano et al., 2016c). Further, the area affected by interrill erosion within the hydrological unit was clearly distinguished in situ by field observations and mapping (Quijano et al., 2014). The hydrological unit was characterized by a contrasting morphology of the land surface associated with the development of a gully system that drains the hydrological unit into the ephemeral stream (Fig.1a). The elevation and the slope in the study field decreased from north to south. The average values of elevation and slope are 632.2 m a.s.l and 6.6%, respectively (Fig. 1b). The slope facing is characterized by northeast - east and south – southeast directions (Fig. 1c). The hydrological unit can be divided into two main physiographic parts with a difference in elevation of 9m between the upper and the lower part of the slope representing erosion and deposition sites, respectively (Fig. 1a). The upper part of the hydrological unit is a relatively flat interrill area and the lower part is characterized by a relatively concave area where the ephemeral gully is well developed, with the occurrence of a depositional fan after intense rainfall events (Quijano et al., 2016b). The upslope and downslope areas were 80m apart and had slope values of 9.8% to 3.2%, respectively (Figs. 1a and b). The cultivated study soils are developed on Quaternary alluvial deposits and are classified as Calcisols according to Quijano et al. (2016a). Soils are alkaline and

nonsaline with mean values of pH and electrical conductivity (EC) of 8.2 and 0.18 dSm−1, respectively, low in organic matter content (≤2.6%) and relatively high in carbonate content (ca. 40%) (Quijano et al., 2016b). In addition, a flat and uncultivated adjacent area where water runoff and associated soil erosion cannot be originated was identified by Quijano et al. (2016b) as stable and undisturbed (not affected by deposition or erosion processes). This elevated landscape position located near the selected field and under Mediterranean original vegetation cover (Quercux ilex L., Rosmarinus officinalis L., Lygeum spartum (L.) Kunth and Thymus vulgaris L.) was selected to compare the particle size distribution according to the settling velocity and the carbon distribution between uncultivated and undisturbed and cultivated Calcisols for analyzing the effect of interrill erosion on soil particles and carbon spatial variability. Uncultivated and undisturbed soils are shallow and are classified as Calcisols. They are alkaline (mean pH=7.4) and non-saline with a maximum value of EC of 0.44 dSm−1 and a mean carbonate content of 28% (Quijano et al., 2016b).

2.2 Experimental design and laboratory analysis

The interrill area represents around 50% of the total area of the hydrological unit. The sampling density was established to be adequate for capturing the variability of SOC and SIC within the study area. Erosion (409m2) and deposition sites (427m2) at the two contrasting slope positions were identified by 137Cs inventories (Quijano et al., 2016b). The first 5 cm depth of soil were sampled because soil redistribution processes by water erosion are more intense in this upper part of the cultivated soil profile. Ten topsoil sampling points were established within the interrill area and three replicates per sampling point were collected randomly at the two contrasting slope positions by using a 4 cm diameter hand-operated core driller (Fig.1a). After sampling, composite samples

were prepared by mixing a subsample of each replicate. Roots and visible plant remains were removed manually and topsoil samples were air-dried at 35 °C during 72 h and passed through a 2-mm sieve to eliminate plant residues, roots and stones (> 2 mm). The>2mm fraction was manually and thoroughly cleaned by brushing to remove fine soil particles and soil aggregates to be included in the ≤2mm fraction for laboratory analyses (Quijano et al., 2016c). In addition, ten sampling points of uncultivated and undisturbed soil were collected up to 25 cm depth in the vicinity of the cultivated field (Fig.1a) by using a 7.2 cm diameter automated core-driller. The sample depth collection was at the same depth as cultivated study soils were ploughed (25 cm) for the last 150 years. Tillage practices have homogenized the soil within the first 25 cm by mixing it thoroughly altering vertical distribution of soil properties (Quijano et al., 2017). Soils were air-dried at room temperature (25 °C) and passed through a 2-mm sieve to separate>2mm and soil fine fraction (≤2 mm). Soil analyses were carried out on fine soil fraction.

2.3 Particle size analysis

Aggregation assembles different size of soil particles into a larger architecture. Such mixtures impede resolving which particles build aggregates (Schweizer et al., 2019). The particle size analysis is a method of separating soils into different fractions. These different sizes of particles present in the soil have different sedimentation and settling behavior, and are influenced by the degree of aggregation (Kaur and Fanourakis, 2016). We analyze soil texture and size information to analyze soil structure and natural aggregation of the study soils with implications for its settling behavior. A first set of particle-size distribution (PSD) measurements was performed on pre-treated samples using both a chemical dispersant (10 ml, sodium hexametaphosphate) and sufficient

mechanical disruption to overcome forces holding aggregates together (Raine, 1998). A second set of PSD measurements was carried out on the same soil samples without adding a dispersing agent to minimize sample disturbance. Particle-size distributions were measured from wet dispersion using a laser diffraction particle size analyzer Malvern Mastersizer 2000 (Malvern Instruments Ltd., UK) operating in the range of 0.02–2000 μm. Particle size was calculated on a volume basis using the Fraunhofer theory (de Boer et al., 1987). The particle size distributions data were divided into 8 categories of particle sizes according to ISO 14688-1:2002. In the ISO system soil material less than 2 μm is considered as clay. Silt consists of three class sizes: fine silt (2–6.3 μm), medium silt (6.3–20 μm) and coarse silt (20–63 μm). Sand is distinguished into the following classes: very fine sand (63–125 μm), fine sand (125–200 μm), medium sand (200–630 μm) and coarse sand (630–2000 μm). The particle size mode for calculating the size distribution was set by default as the general purpose and the particle shape was set to spherical (Malvern Instruments Ltd, 2007). The suspending medium during analysis was distilled water with a refractive index of 1.33. The sonication time was five minutes using an ultrasonic probe with a maximum power of 35W and a frequency of 40 kHz. The amplitude of the displacement was 20 μm. The pump and stirrer speeds selected for the dispersion unit of the Hydro 2000 G, (Malvern Instruments Ltd., UK) were 900 rpm and 2300 rpm, respectively. The speed was set at its maximum 2500 rpm for the pump and 1000 rpm for the stirrer. According to Sperazza et al. (2004) and Storti and Balsamo (2009), a pump speed between 2000–2300 rpm should ensure the re-circulation of coarser materials, without significantly reducing the precision of the finer grains. During the second set of PSDs measurements soil samples were directly introduced into the dispersion unit and the pumping/stirring speed were 700 rpm and 1700 rpm, respectively. Soil particle size analysis on pre-

treated soils were compared with the non-pre-treated soils to analyse the effect of aggregate breakdown by chemical and mechanical dispersion and the degree of soil aggregation on the study soils which influence the sedimentation and settling behavior of soils.

2.4 Settling velocity measurements

Sedimentation has been a standard methodology for particle size analysis since the early 1900s (Fisher et al., 2017). Settling velocity tube is a sedimentation instrument proposed by Owen (1976) is a useful tool to fractionate soil by the extraction of an established number of samples at specific times from a vertical tube of water and to obtain distinct samples according to their settling velocity (Malarkey et al., 2013). This method for particle size analysis which can be used in soil erosion modelling (Jetten et al., 2003; Jiménez and Madsen, 2003) provides information on the soil structure and aggregate wettability (Hu et al., 2013a). Soil fractionation by sedimentation was carried out in the laboratory of the Physical Geography and Environmental Change Research Group of the University of Basel by using 1.8m long settling tube apparatus. This device enables the collection of soil subsamples at specific time increments to estimate particle size. The settling tube is mounted in a vertical position and has an internal diameter of 5 cm. The ratio of the diameter of the tube to finer soil particles of ≤2mm diameter is approximately 25 to 1. This large ratio eliminates concerns with edge effects that could be expected to introduce errors of<10% (Lovell and Rose, 1988a, b). The settling tube consists of four components (Fig.1d): i) the settling tube in which soil particles settle through a static fluid (i.e. water), ii) the injection device to introduce the soil sample into the settling tube, iii) the turntable in which the collection of the soil subsamples is carried out at different settling time (Fig.1e) and iv) the control panel to

establish the rotational speed and resting/moving intervals of the turntable. A more detailed description of the settling tube is included in Hu et al. (2013a). The settling velocity tube is based on mathematical models such as the Stoke's Law for spherical particles in the low Reynolds number regime and its derivates (e.g. Hallermeier, 1981; Van Rijn, 1993; Ferguson and Church, 2004). To deal with the irregular and nonspherical soil particle's geometry, we used the concept of equivalent quartz size (EQS) employed in most particle-sizing techniques (Hu et al., 2013b; Hu and Kuhn, 2016). An equivalent grain size represents the diameter of a spherical sand particle that may be related to any regular geometry for the conversion of equivalent quartz size classes to settling velocities. Following the protocol by Hu and Kuhn (2016), the five EQS classes were converted to five settling velocities and corresponding settling times using Stokes' Law (Table 1). In this study, five settling classes were established to fractionate the cultivated and uncultivated soil samples (> 250 μm, 125–250 μm, 63–125 μm, 32–63 μm and<32 μm). These five particle size classes were selected because they correspond to the conventional classes used for sieving sand, i.e. enabling the equivalent quartz size approach (Hu and Kuhn, 2014) (Table 1). In addition, after fractionation, these five classes allowed us to obtain enough soil at each size class for carbon measurements and analysis. Prior to placing the soil subsample into the settling tube, a subsample of 25 g of dry soil (≤2mm fraction) was immersed into 50 ml of distilled water for 15 min. This slow-wetting emphasizes aggregate breakdown by the compression of entrapped air during wetting (slaking) (Le Bissonnais, 1996). To explore the simplicity of the settling velocity test in terms of reduced sample preparation to avoid the proposed soil pre-treatment (slow-wetting) by Hu et al. (2013a) and to study the effect of slow wetting on the settling behavior, we tested the possibility to introduce into the settling tube apparatus non-pre-wetted soil subsamples (25 g).

2.5 Soil and statistical analyses

After settling, all the soil fractions (n=200) were dried at 40 °C and weighed. The contents (g kg−1) of SOC and SIC in each of the settling size classes were determined by dry combustion method (Wright and Bailey, 2001) using a multiphase carbon analyzer LECO RC-612 at 550 °C and 950 °C, respectively (LECO Corp., St. Joseph, MI, USA). In addition, the SOC and SIC mass (mg g−1) in each of the size classes was calculated by multiplying the dry weight collected in each class with the concentration of soil organic and inorganic carbon, respectively. Statistical analysis was carried out using the SPSS 19.0 (IBM-SPSS, Inc., USA). The assumption of normality was checked by using the Shapiro-Wilk test. The log transformation was used, when the results of the normality test for data were lower than 0.05, to transform skewed data to approximately conform to normality and then perform the parametric test on the transformed data (Quijano et al., 2019). One-way analysis of variance (ANOVA) tests were appropriated to check for significant differences in the percentages of particle size ranges among the treatments (one categorical factor). We compared the particle size distributions between dispersed and non-dispersed samples and the settling velocity distributions of pre-wetted and non pre-wetted samples at each aggregate size fraction. When significant differences ($p \leq 0.05$) were observed, multiple comparisons of means were performed with Fisher's least significant difference (LSD) test. A two-way ANOVA procedure was used to determine the effect of the topographic position and soil redistribution (erosion, stable and deposition) on the particle size class and associated SOC and SIC. The significance of main effects was determined based on type III sum of squares and was expressed in terms of Pearson correlation coefficients. When a statistically significant interaction ($p \leq 0.05$) was reported multiple comparisons were carried out. These post hoc tests were based on LSD test.

3. Results

3.1. Particle size distribution

Most uncultivated soil had loam texture, in which silt and sand were the predominant particle size fractions and clay content was less than 10%. Cultivated soils with silt loam texture had lower values of sand compared to uncultivated soil (Fig. 2). Before dispersion, uncultivated and cultivated downslope soils had relatively coarse texture with a predominance of medium sand compared to cultivated upslope soil where the coarse silt fraction had the highest mean value (Fig. 2). After dispersion, there was a clear effect of aggregate breakdown on the particle size distribution as shown in Fig. 2. A significant difference was found ($p \leq 0.05$) between the mean values in dispersed (D) and nondispersed (ND) samples for each fraction in uncultivated and cultivated soils, apart from the mean values of coarse sand fraction in the cultivated upslope soil and coarse silt in the cultivated downslope soil (Table 2). The difference between the particle size (%) of the non-dispersed and dispersed soils was lower in cultivated downslope soil compared to cultivated upslope soil and uncultivated soils (Fig. 2). The ultrasonic dispersion and chemical pretreatment led to a shift in particle size distribution increasing significantly ($p \leq 0.05$) the ≤63 μm fraction in uncultivated soil and the≤20 μm fraction in cultivated soil whereas the percentage of sand decreased significantly in uncultivated and cultivated upslope soil.

3.2. Soil particle size distribution from settling velocity data

Results from ANOVA analysis to compare the mass distribution of the five settling size classes between the prewetted (P) and non-prewetted (NP) soil samples indicated that the initial moisture content of the aggregates did not influenced their settling behavior and water stability. There wasn’t a significant difference between the mean of the mass

collected at each settling size class in P and NP soil samples (Table 3). The aggregate breakdown due to the prewetting of dry aggregates was negligible. Therefore, only the soil fractionation results from pre-treated soil samples are presented. The cumulative distribution of weight (g) of soil particles deposited as a function of sedimentation time indicated that the settling behavior varied by topographic position (Fig. 3). Most of the soil mass was collected within the first 10 min of settling ranging from 64% for the cultivated upslope soil to 75% from the uncultivated soil. The curves of all three soils flattened after ten minutes (Fig. 3). In the uncultivated soil, the ≥250 μm fraction accumulated the greatest mass with a mean value of 29% whereas cultivated soil was considerably and significantly depleted in this fraction from two to four times at downslope and upslope sampling sites, respectively, compared to uncultivated soil (Fig. 4). In cultivated soil, most of the settled soil particles were comprised between 63 μm and 125 μm ranging from 30% to 44% of the soil sample total mass whereas in uncultivated soil the mean percentage of mass was statistically significantly ($p \leq 0.05$) lower. The cultivated upslope

3.3 Soil organic and inorganic carbon concentration in size-class

The average SOC mass was ∼1.8 times higher in uncultivated soils (8.6 ± 2.9 mg g−1) than in cultivated upslope (4.9 ± 2.5 mg g−1) and downslope soils (3.7 ± 1.7 mg g−1). The analysis of the SOC distribution within different particle (mineral and aggregated) size fractions in soils showed that the content of SOC was not distributed uniformly across all size classes. The two-way ANOVA confirmed significant differences ($p \leq 0.05$) among the SOC means between slope position and particle size classes (Table 4). From the multiple comparison procedure it was determined that means of SOC content in uncultivated soil were significantly higher from those in cultivated soil within

the same settling size class at the 95.0% confidence level. In uncultivated soil, the SOC content (g kg−1) had the highest values in the finer particles (≤63 μm) compared to the other settling size classes where SOC (g kg−1) decreased in the following order:>250 μm, 125–250 μm and 63–125 μm (Fig. 5). More than 50% of the SOC was associated with finer soil particles in uncultivated compared to cultivated soil. In cultivated soil, the trends in the distribution of SOC content across the settling size classes showed an opposite pattern at the different slope positions. A higher SOC content was associated with the ≤ 63 μm fraction in the cultivated downslope soil whereas in cultivated upslope soil the highest amount of SOC content was found in the>125 μm fraction (Fig. 5). SOC associated with>125 μm fraction was lower downslope than upslope position. SOC contents associated with 63–125 μm settling size class did not change at different slope positions. The mean percentage of SIC slightly increased in parallel with the settling size class (Fig. 6) predominating in the coarse size particles mainly in cultivated downslope soil. The two-way ANOVA confirmed significant differences ($p \leq 0.05$) among the SIC means between slope position and settling size classes (Table 5). From the multiple comparison procedure it was determined that means of SIC content in uncultivated soil were significantly different from cultivated soil within the same settling size class at the 95.0% confidence level. On average, in uncultivated soil, the concentration of SIC was lower (16.3 ± 6.8 mg g−1) than in cultivated upslope (21.4 ± 12.9 mg g−1) and downslope soils (24.5 ± 12.5 mg g−1). In uncultivated soil, the content of SIC did not vary between the different settling size classes. By comparing cultivated soil at the different slope positions, the mean values of SIC at each size class were higher at downslope compared to upslope position. The coarsest particles (with the largest diameter) were associated with higher contents of SIC in cultivated downslope soil.

4. Discussion

4.1 Soil particle aggregation and soil carbon distribution

In our study, the impact of the chemical and physical dispersion on soils vary between cultivated and uncultivated soils (i.e. SOC content) and slope position (i.e. soil redistribution process) which is recognised in the analysis of the particle size distributions. The degree of soil aggregates was observed by the reduction in the amount of the sand size fraction (≥63 μm) and the subsequent increase in smaller sized fractions due to dispersion. After dispersion, the increase of the ≤20 μm fraction is more evident in cultivated upslope soil compared to the downslope position suggesting that the dispersibility and disaggregation of soil particles was higher and more effective at upslope position. The dispersibility of soil aggregates is related to its aggregate stability which has been used to indicate soil resistance to erosive agents and soil quality (Nichols and Toro, 2011). Particle size distribution (PSD) is considered one of the most important physical properties of soil and was used to investigate the detachment and transport mechanisms involved in sediment movement. Ding and Huang (2017) demonstrate that considering each particle size separately rather than use only the total sediment in assessing interrill erosion processes is more useful for erosion modelling.

Previous studies reported that the overland flow transportability and the subsequent deposition process depended on the PSD (Martínez- Mena et al., 2002). A better understanding of the sediment PSD will improve understanding of erosion processes, which in turn will improve erosion modelling (Asadi et al., 2011). Furthermore, several studies suggest that changes in PSD can provide useful insights on the influences of land managament on degraded systems (Deng et al., 2017; Su et al., 2004). The decrease of aggregates in cultivated compared to uncultivated soils was observed by the fact that medium and coarse sand contents (200–2000 μm) were greater in uncultivated

soil (40%) than in cultivated soil at upslope (16%) and downslope (33%) positions. These trends in soil aggregation indicate that soil aggregate stability and organic carbon are closely related in the study soils. The>250 μm fraction contain more SOC in uncultivated than in cultivated soil as has been shown by several authors (Cambardella and Elliott, 1993; Hontoria et al., 2016). According to Liu et al. (2014) the direct consequence of the aggregate hierarchy is an increase in carbon content as it was reported in the uncultivated soil, since the>250 μm fraction is composed of smaller aggregate-size classes in combination with organic binding agents increasing aggregate-size class and organic carbon.

On the other hand, cultivation leads to the depletion of SOC compared to uncultivated soil as found in a previous research in the study area (Quijano et al., 2016b). This resulting depletion of SOC and deterioration of soil structure in cultivated soil samples can be related to the effect of tillage practices conducted in the study field for the last 150 years. Similar results were found by Six et al. (2000) who reported that ploughing induced modifications of soil physical properties resulting in damage to soil structure in the top 5 cm of soil from a longterm agricultural field. Pagliai et al. (2004) also concluded that a better aggregation plays an important role in preventing soil crust formation thus diminishing soil erosion. The reason appears to be that the detached soil particles by rapid wetting settle into pores causing surface sealing and reducing infiltration (Amezteka et al., 2004). Thus, soil organic compounds may influence the stability and formation of soil aggregates by binding soil mineral particles into Macroaggregates (Malo et al., 2005), which would influence the mechanical strength of soil aggregates limiting the slaking effect during wetting (Sullivan, 1990).

According to Reichert et al. (2001), the rapid wetting of air-dried sediment causes a general decrease in aggregate settling velocities attributed to the breakdown of the

coarser aggregates. This effect was found in uncultivated and cultivated upslope soils where the role of SOC as an aggregating agent was evident. However, in cultivated downslope soil, the highest content of soil inorganic carbon mainly in macroaggregates along with little dispersed coarse sized particles points to the existence of lithogenic or/and secondary carbonates as binding agents. After settling, the proportion of water-stable Macroaggregates (≥250 μm) was significantly affected by the nature of the binding agents (Fig. 3). In agreement with the observations made by Virto et al. (2011), in intensively tilled Mediterranean soils, inorganic carbon content was more important than organic binding agent.

4.2 Particle size selectivity and implication on soil carbon pools

Soil organic carbon is related to finer particles size classes (≤63 μm) with lower settling velocities at the downslope position. This relationship has been reported in other temperate soils by Hassink (1997) and Liang et al. (2009). The preferential mobilization and selective transport of finer and organic-rich soil particles are important processes that affect physical (e.g., water retention) and chemical (e.g., nutrient storage) soil properties (Koiter et al., 2017; Rousseau et al., 2004). Despite the important influence of the transport of aggregates by erosion on associated carbon concentrations in different aggregate size classes this topic has not been thoroughly investigated. Liu et al. (2019) reported that the SOC concentrations of each aggregate size class in sediments were different from those in the original soil and SOC was enriched in sediment particles of different sizes under sheet erosion.

In this study, the higher concentrations of SOC found within the fine-grained fractions coupled with their preferential mobilization and transport result in a lateral redistribution of SOC across the study area. From an environmental point of view and

as shown by other authors, the above combination ends in an increasing significance of erosion (Zhang et al., 2014; Navas et al., 2012; Kuhn et al., 2010).

The lower SOC content in finer size classes in the cultivated soil upslope compared to downslope can be related to a risk of higher erodibility in this part of the study area. The deterioration of soil structure and aggregate stability is linked to SOC content. This finding is in line with Czyz (2002), who demonstrated a reduction of clay dispersability with increasing SOC.

The accumulation of SIC at downslope position is in agreement with the findings of Kolesár and Čurlik (2015) who reported that topography-induced spatial heterogeneity influences the distribution of carbonates and therefore SIC stocks along toposequences. They stated that spatial variability of carbonates within the soil profile is closely related to the major movement flow through the landscape.

Carbonate enrichment at downslope positions involves the process of dissolution of carbonates in the upper sections of soils and transportation which is followed by re-precipitation during drying of the soil (Wu et al., 2009). In our soils the SOC to SIC ratio in the >250 μm settling size class increased from 0.5 in cultivated upslope soil to 0.8 in downslope soil suggesting an enrichment of SIC across the slope in this fraction. The increase of SIC related with coarse settling size classes may be due to precipitation of pedogenic carbonates (secondary calcium carbonate) that forms coatings around primary particles and organic residues, enhancing aggregation (Fernández-Ugalde et al., 2011) and leading to significantly coarser textures (Lucke and Schmidt, 2015). Furthermore, Quijano et al. (2019) found strong, direct and significant correlation between the percentage of water-stable aggregates and SIC content in cultivated Calcisols related with the role of carbonates to act as a binding agent (Virto et al., 2011).

Furthermore, the observed increase of coarse settling size classes (≤125 μm) in downslope soil may be due to the effect of sorting process as reported in a previous study by Quijano et al. (2016b) in this cultivated area. Field observations evidenced that selective removal of finer soil particles and deposition of coarse sediments occurred at the end of the ephemeral gully when the transport capacity of runoff decreased. Interrill erosion can be highly selective at low flow rates and it may help to explain selective soil carbon erosion and determine the fate of the eroded carbon in Mediterranean Calcisols.

5. Conclusions

This study showed that at field scale, particle size distribution was a function of soil texture and slope position in Mediterranean Calcisols. The different distribution of the settling size classes revealed sorting processes and preferential transport of fine particles from upslope to downslope by runoff. SOC was predominantly concentrated in the finer size classes (≤63 μm) with smaller settling velocities contrary to SIC that accumulated in coarse soil particles at downslope position. The predominance of macroaggregates at downslope could be attributed to the considerable accumulation of secondary carbonates in these topsoils. This trend differed from uncultivated soils with lower SIC content, in which the fine-grained was relatively enriched in organic carbon-rich particles. Our results highlighted the importance of considering the inorganic carbon in secondary carbonate-rich topsoil for analyzing soil size particles and carbon distribution, which has been under studied to date.

This study reported that settling velocity distributions could be a useful tool for assessing changes in soil aggregation and for identifying causal mechanisms in relation to soil and carbon mobility in an interrill area. This method may be used for a better

prediction and process-based understanding of the redistribution of eroded sediment and associated soil carbon across landscapes.

Acknowledgements

This work was funded by the CICYT project (CGL2014-52986-R).

References

Álvaro-Fuentes, J., Cantero-Martínez, C., López, M.V., Paustian, K., Denef, K., Stewart, C.E., Arrúe, J.L., 2009. Soil aggregation and soil organic carbon stabilization: effects of managements in semiarid Mediterranean agroecosystems. Soil Sci. Soc. Am. J. 73, 1519–1529.

Amezteka, E., Aragües, R., Gazol, R., 2004. Infiltration of water in disturbed soil columns as affected by clay dispersión and aggregate slaking. Span. J. Agric. Res., 2(3), 459–471.

Angulo-Martínez, M., Beguería, S., Navas, A., Machín, J. 2012. Splash erosion under natural rainfall on three soil types in NE Spain. Geomorphology, 175- 176, 38–44.

Asgari Hafshejani, N., Jafari, S. (2017). The study of particle size distribution of calcium carbonate and its effects on some soil properties in khuzestan province. Iran Agricultural Research, 36(2), 71–80.

Ballabio, C., Borrelli, P., Spinoni, J., Meusburger, K., Michaelides, S., Beguería, S., Klik, A., Petan, S., Janeček, Olsen, P., Aalto, J., Lakatos, M., Rymszewicz, A., Dumitrescu, A., Perčec-Tadić, M., Diodato, N., Kostalova, J., Rousseva, S., Banasik, K., Alewell, C., Panagos, P., 2017. Mapping monthly rainfall erosivity in Europe. Sci. Total Environ. 579, 1298–1315.

Barreiro-Lostres, F., Moreno, A., González-Sampériz, P., Giralt, S., Nadal-Romero, E., Valero-Garcés, B., 2017. Erosion in Mediterranean mountain landscapes during the last millennium: a quantitative approach based on lake sediment sequences (Iberian Range, Spain). Catena, 149, 782–798.

Beguería S, Angulo-Martínez M, Gaspar L, Navas A. 2015. Detachment of soil organic carbon by rainfall splash: Experimental assessment on three agricultural soils of Spain. Geoderma 245-246: 21-30.

Berhe, A.A., Harte, J., Harden, J.W., Torn, M.S., 2007. The significance of the erosion induced terrestrial carbon sink. Bioscience 57 (4), 337–346.

Berhe, A. A., J. W. Harden, M. S. Torn, M. Kleber, S. D. Burton, and J. Harte (2012), Persistence of soil organic matter in eroding versus depositional landform positions, J. Geophys. Res., 117, G02019.

Berhe, A. A., Arnold, C., Stacy, E., Lever, R., McCorkle, E., Araya, S. N., 2014. Soil erosion controls on biogeochemical cycling of carbon and nitrogen. Nature Education Knowledge 5(8), 2.

Borrelli, P, Robinson, D.A., Fleischer, L.R., Lugato, E., Ballabio, C., Alewell, C., Meusburger, K., Modugno, S., Schütt, B., Ferro, V., Bagarello, V., Van Oost, K., Montanarella, L., Panagos, P. 2017. An assessment of the global impact of 21st century land use change on soil erosion. Nat Commun. 8(1), Art. 2013.

Bremenfeld, S., Fiener, P., Govers, G., 2013. Effects of interrill erosion, soil crusting and soil aggregate breakdown on in situ CO2 effluxes. Catena 104, 14 – 20.

Cambardella, C.A., Elliott, E.T., 1993. Carbon and nitrogen distribution in aggregates from cultivated and native grassland soils. Soil Sci. Soc. Am. J., 57(4), 1071–1076.

de Boer, G. B. J., de Weerd, C., Thoenes, D., and Goossens, H. W. J., 1987. Laser diffraction spectrometry: Fraunhofer diffraction versus Mie scattering. Particle Characterization 4, 138–146.

Deng, Y., Cai, C., Xia, D., Ding, S., Chen, J. 2017. Fractal features of soil particle size distribution under different land use patterns in the alluvial fans of collapsing gullies in the hilly granitic region of souther China. *PLoS ONE*. 12(3), e0173555

Ding, W., Huang, C. 2017. Effects of soil surface roughness on interrill erosion processes and sediment particle size distribution. Geomorphology 295, 801 – 810.

Dong, X., Qiuyu, H., Guitong L., Qimei, L., Xiaorong, Z. 2017. Contrast effect of long-term fertilization on SOC and SIC stocks and distribution in different soil particle-size fractions. J. Soils Sediments. 17, 1054–1063.

Ferguson, R. I., Church, M., 2004. A simple universal equation for grain settling velocity. J. Sediment. Res. 74(6), 933–937.

Fernández-Ugalde, O., Virto, I., Barré, P., Gartzia-Bengoetxea, N., Enrique, A., Imaz, M.J., Bescansa, P., 2011. Effect of carbonates on the hierarchical model of aggregation in calcareous semi-arid Mediterranean soils. Geoderma 164, 203 – 214.

Fisher P, Aumann C, Chia K, O'Halloran N, Chandra S., 2017. Adequacy of laser diffraction for soil particle size analysis. Docoslis A, ed. *PLoS ONE*. 12(5), e0176510.

Gaspar & Navas 2013. Vertical and lateral distributions of ^{137}Cs in cultivated and uncultivated soils on Mediterranean hillslopes. Geoderma 207-208, 131-143.

Gaspar, L., Quijano, L., Lizaga, I., Navas, A. 2019. Effects of land use on soil organic and inorganic C and N at ^{137}Cs traced erosional and depositional sites in mountain agroecosystems. Catena, DOI: 10.1016/j.catena.2019.05.004

Hallermeier, R. J., 1981. Terminal settling velocity of commonly occurring sand grains. Sedimentology 28, 859–865.

Hassink, J., 1997. The capacity of soils to preserve organic C and N by their association with clay and silt particles. Plant Soil 191, 77–87.

Hontoria, C., Gómez-Paccard, C., Mariscal-Sancho, I., Benito, M., Pérez, J., Espejo, R., 2016. Aggregate size distribution and associated organic C and N under different tillage systems and Ca-amendment in a degraded Ultisol. Soil Till. Res. 160, 42–52.

Hu, Y., Fister,W., Rüegg, H.R., Kinnell, P.A., Kuhn, N.J., 2013a. The use of equivalent quartz size and settling tube apparatus to fractionate soil aggregates by settling velocity. Geomorphology Techniques (Online Edition), British Society for Geomorphology Section–1.

Hu, Y., Fister, W., Kuhn, N.J., 2013b. Temporal variation of SOC enrichment from interrill erosion over prolonged rainfall simulations. Agriculture 3, 726–740.

Hu, Y., Kuhn, N. J., 2014. Aggregates reduce transport distance of soil organic carbon: are our balances correct?, Biogeosciences, 11, 6209–6219.

Hu, Y, Kuhn, N.J., 2016. Erosion-induced exposure of SOC to mineralization in aggregated sediment. Catena 137, 517–525.

Issa, O.M., Le Bissonnais, Y., Planchon, O., Favis-Mortlock, D., Silvera, N., Wainwright, J., 2006. Soil detachment and transport on field- and laboratory-scale interrill areas: ersion processes and the size-selectivity of eroded sediment. Earth Surf. Process. Landforms 31, 929–939.

Jetten, V., Govers, G., Hessel, R., 2003. Erosion models: quality of spatial predictions. Hydrol. Process. 17, 887–900.

Jiménez, J.A., Madsen, O.S., 2003. A simple formula to estimate settling velocity of natural sediments. J. Waterw. Port C-ASCE 129, 70–78.

Kaur A, Fanourakis GC. 2016. The effect of type, concentration and volume of dispersing agent on the magnitude of the clay content determined by the hydrometer analysis. J. S. Afr. Inst. Civ. Eng. 58(4), Art. #1376.

Koiter, A.J., Owens, P.N., Petticrew, E.L., Lobb, D.A., 2017. The role of soil surface properties on the particle size and carbon selectivity of interrill erosion in agricultual landscapes. Catena 153, 194–206.

Kolesár, M., Čurlik, J. 2015. Origin, distribution and transformation of authigenic carbonates in loessic soils. Eurasian Journal of Soil Science 4 (2015) 38 - 43

Kuhn, N.J., Hoffmann, T., Schwanghart, W, Dotterweich, M., 2009. Agricultural soil erosion and global carbon cycle: controversy over?. Earth Surf. Proc. Land. 34, 1033–1038.

Kuhn, N.J., 2010. Rainfall simulation experiments on crusting and interrill sediment organic matter content on a silt loam from Devon. Die Erde : Zeitschrift der Gesellschaft für Erdkunde, Berlin ; Forum für Erdsystem- und Erdraumforschung 141(4), 283–301.

Kuhn, N.J., Armstrong, E.K., 2012. Erosion of organic matter from sandy soils: Solving the mass balance. Catena 98, 87 – 95.

Kuhn, N.J., Van Oost, K., Cammeraat, E., 2012a. Soil erosion, sedimentation and the carbon cycle. Catena, 94, 1–2.

Kuhn, N.J., Armstrong, E.K., Ling, A.C., Connolly, K.L., Heckrath, G., 2012b. Interrill erosion of carbon and phosphorus from conventionally and organically farmed Devon silt soils. Catena 91, 94–103.

Lal, R., 2005. Soil erosion and carbon dynamics. Soil Till. Res. 81, 137–142.

Lasanta, T., Beguería, S., García-Ruíz, J.M., 2006. Geomorphic and hydrological effects of traditional shifting agriculture in a Mediterranean mountain area, Central Spanish Pyrenees. Mt. Res. Dev. 26(2), 146–152.

Le Bissonnais, Y. 1996. Aggregate stability and assessment of soil crustability and erodibility: I. Theory and methodology. European J. Soil Sci. 47, 425-437.

Liang, A.Z., Yang, X., Zhang, X., McLaughlin, N., Shen, Y., Li, W., 2009. Soil organic carbon changes in particle-size fractions following cultivation of Black soils in China. Soil Till. Res.105(1), 21–26.

Liu, L., Li, Z., Xiao, H.B., Wang, B., Nie, X.D., Liu, C., Ni, L.S. Wang, D.Y. 2019. The transport of aggregates associated with soil organic carbon under the rain-induced overland flow on the Chinese Loess Plateau. Earth Surf. Process. Landforms. 44, 1895-1909.

Lizaga, I., Quijano L., Gaspar, L., Raños, M.C., Navas, A. 2019. Linking land use changes to variation in soil properties in a Mediterranean mountain agroecosystems. Catena 172, 516–527.

Lizaga, I., Quijano L., Gaspar, L., Navas, A. 2018. Estimating soil redistribution patterns with ^{137}Cs measurements in a Mediterranean mountain catchment affected by land abandonment. Land Degrad. Dev. 29(1), 105–117.

Lizaga I, Quijano L, Palazón L, Gaspar L, Navas A. 2017. Enhancing connectivity index to assess the effects of land use changes in a Mediterranean catchment. Land Degrad Dev. 29(3), 663–675.

Loch, R.J. 2001. Settling velocity – a new approach to assessing soil and sediment properties. Comput. Electron. Agric. 31, 305–316.

Lovell, C.J., Rose, C.W., 1988a. Measurement of soil aggregate settling velocities. I. A modified bottom withdrawal tube method. Aust. J. Soil Res. 26, 55–71.

Lovell, C.J., Rose, C.W., 1988b. Measurement of soil aggregate settling velocities. II. Sensitivity to sample moisture-content and implications for studies on structural stability. Aust. J. Soil Res. 26, 73–85.

Lucke, B. Schmidt, U. 2015. Grain size analysis of soils in semi-arid regions: with or without calcium carbonate removal, and which device should be chosen?. Grain size analysis of calcareous soils and sediments. Erlanger Geographische Arbeiten Band 42, 83–98.

Malarkey, J., Jago, C.F., Hübner, R., Jones, S.E., 2013. A simple method to determine the settling velocity distribution from settling velocity tubes. Cont. Shelf Res. 56, 82–89.

Malo, D.D., Schumacher, T.E., Doolittle, J.J., 2005. Long-term cultivation impacts on selected soil properties in the northern great Plains. Soil Till. Res. 81, 277–291.

Malvern Instruments Ltd. 2007. Mastersizer 2000 User manual. MAN0384 Issue 1.0.

Mantovanelli, A., Ridd, P.V., 2006. Devices to measure settling velocities of cohesive sediment aggregates : a review of the in situ technology. J. Sea Res. 56, 199–226.

Martí-Roura, M., Hagedorn, F., Rovira, P., Romanyà, J. 2019. Effect of land use and carbonates on organic matter stabilization and microbial communities in Mediterranean soils. Geoderma 351, 103 – 115.

Martínez-Mena M, Castillo V, Albaladejo J. 2002. Relationships between interrill erosion processes and sediment particle size distribution in a semiarid Mediterranean área of SE of Spain. Geomorphology 45(3-4), 261–275.

Meyer, L.D., Foster, G.R.,Romkens, M.J.M.., 1975.Mathematical simulation of upland erosion using fundamental erosion mechanics. Proc. of Sediment Yield Workshop, USDA Sedimentation Laboratory, Oxford, Miss. ARS-S-40, 177–189.

Navas, A., Gaspar, L., Quijano, L., López-Vicente, M., Machín, J. 2012. Patterns of soil organic carbon and nitrogen in relation to soil movement under different land uses in mountain fields (South Central Pyrenees). Catena, 94, 43–52.

Navas, A., López-Vicente, M., Gaspar, L., Machín, J. 2013. Assessing soil redistribution in a complex karst catchment using fallout ^{137}Cs and GIS. Geomorphology 196, 231–241.

Navas, A., López-Vicente, M., Gaspar, L., Palazón, L., Quijano, L. 2014. Establishing a tracer-based sediment budget to preserve wetlands in Mediterranean mountain agroecosystems (NE Spain). Science of the Total Environment, 496, 132–143.

Navas, A., Machín, J., Beguería, S., López-Vicente, M., Gaspar. L. 2008. Soil properties and physiographic factors controlling the natural vegetation re-growth in a disturbed catchment of the Central Spanish Pyrenees. Agroforestry Systems, 72(3), 173–185.

Navas, A., Quine, T.A., Walling, D.E., Gaspar, L., Quijano, L., Lizaga, I. 2017. Relating intensity of soil redistribution to land use changes in abandoned Pyrenean fields using fallout caesium-137. Land Degradation and Development. 28, 2017–2029

Nichols, K.A., Toro, M., 2011. A whole soil stability index (WSSI) for evaluating soil aggregation. Soil Till. Res. 111, 99–104.

Nimmo, J.R. 2013. Aggregation: Physical Aspects. Encyclopedia of Soils in the Environment, 2005, 28–35.

Owen, M.W., 1976. Determination of the settling velocities of cohesive muds. Hydraulic Research Station, Wallingford, Report No. IT 161, pp. 1–8.

Pagliai, M., Vignozzi, N., Pellegrini, S., 2004. Soil structure and the effect of management practices. Soil Till. Res. 79, 131–143.

Panagos, P., Imeson, A., Meusburger, K., Borrelli, P., Poesen, J., Alewell, C., 2016. Soil conservation in Europe: wish or reality? Land Degrad. Dev. 27, 1547–1551.

Papanicolaou, A. N., K. M. Wacha, B. K. Abban, C. G. Wilson, J. L. Hatfield, C. O. Stanier, and T. R. Filley (2015), From soilscapes to landscapes: A landscape-oriented approach to simulate soil organic carbon dynamics in intensively managed landscapes, J. Geophys. Res. Biogeosci.

Pimentel, D., Harvey, C., Resosudarmo, P., Sinclair, K., Kurz, D., Mcnair, M., Crist, S., Sphpritz, L., Fitton, L., Saffouri, R., Blair, R., 1995. Environmental and economic costs of soil erosion and conservation benefits. Science, 267, 1117–1123.

Quijano, L., Chaparro, M.A.E., Marié, D.C., Gaspar, L., Navas, A., 2014. Relevant magnetic and soil parameters as potential indicators of soil conservation status of Mediterranean agroecosystems. Geophys. J. Int. 198(3), 1805–1817.

Quijano, L., Gaspar, L., Navas, A., 2016a. Lateral and depth patterns of soil organic carbon fractions in a mountain Mediterranean agrosystem. J. Agr. Sci. 154, 287–304.

Quijano, L., Gaspar, L., Navas, A., 2016b. Spatial patterns of SOC, SON, ^{137}Cs and soil properties as affected by redistribution processes in a Mediterranean cultivated field (Central Ebro Basin). Soil Till. Res. 155, 318–328.

Quijano, L., Beguería, S., Gaspar, L., Navas, A., 2016c. Estimating erosion rates using ^{137}Cs measurements and WATEM/SEDEM in a Mediterranean cultivated field. Catena 138, 38–51.

Quijano, L. Van Oost, K., Nadeu, E., Gaspar, L., Navas, A., 2017. Modelling the effect of land management changes on soil organic carbon stocks in a Mediterraenan cultivated field. Land Degradation and Development 28, 515–523.

Quijano, L., Kuhn, N.J, Navas, A. 2019. Soil particle size distribution and induced soil

carbon transport by ephemeral gully erosion in Mediterranean mountain arable land. Earth Surf. Process. Landforms. DOI: 10.1002/esp.4703

Raine S.R. Towards a fundamental understanding of soil aggregate breakdown under applied mechanical energies. Proc. Int. Conf. Eng. in Agriculture; Perth, Australia. September 27-30.1998.

Razafimbelo, T.M., Albrecht, A., Oliver, R., Chevallier, T., Chapuis-Lardy, L., Feller, C., 2008. Aggregate associated-C and physical protection in a tropical clayey soil under Malagasy conventional and no-tillage systems. Soil Till. Res. 98, 140–149.

Reichert, J.M., Schäfer, M.J., Cassol, E.A., Norton, L.D., 2001. Interrill and rill erosion on a tropical sandy loam soil affected by tillage and consolidation, in: Stott, D.E., Mohtar, R.H., Steinhardt, G.C. (Eds.), Sustaining the Global Farm. Selected papers from the 10th International Soil Conservation Organization Meeting, May 24–29, 1999, Purdue University and the USDA-ARS Soil Erosion Research Laboratory, USA.

Rowley, M.C., Grand, S., Verrecchia, É.P., 2018. Calcium-mediated stabilisation of soil organic carbon. Biogeochemistry 137, 27 – 49.

Shi, P., Van Oost, K., Schulin, R., 2017. Dynamics of soil fragment size distribution under successive rainfalls and its implication to size-selective sediment transport and deposition. Geoderma 3008, 104–111.

Six, J., Paustian, K., Elliot, E.T., Combrink, C., 2000. Soil structure and organic matter: I. Distribution of aggregate size classes and aggregate associated carbon. Soil Sci. Soc. Am. J. 64, 681–689.

Sperazza, M., Moore, J.N. and Hendrix, M.S. (2004) High resolution particle size analysis of naturally occurring very fine-grained sediment through laser diffractometry' Journal of Sedimentary Research 74 (5), 736 – 743.

Storti, F. and Balsamo, F. 2009. Particle size distributions by laser diffraction – Part 1: Sensitivity of granular matter strength to analytical operating procedures. Solid Earth Discuss 1, 93–141.

Su YZ, Zhao HL, Zhao WZ, Zhang TH (2004) Fractal features of soil particle size distribution and the implication for indicating desertification. Geoderma 122, 43–49

Sullivan, L.A., 1990. Soil organic matter, air encapsulation and water stable aggregation. J. Soil Sci. 41, 529–534.

Schweizer, S.A., Bucka, F. B., Graf-Rosenfellner, M., Kögel-Knabner, I. 2019. Soil microaggregate size composition and organic matter distribution as affected by clay content. Geoderma, 355, 113901.

Tromp-van Meerveld, H.J., Parlange, J.Y., Barry, D.A., Tromp, M.F., Sander, G.C., Walter, M.T., Parlange, M.B., 2008. Influence of sediment settling velocity on mechanistic soil erosion modeling. Water Resources Research 44, W06401.

Van Rijn, L. C., 1993. Principles of sediment transport in rivers, estuaries and coastal seas. Vol. 1006. Aqua publications Amsterdam.

Van Oost, K. V., G. Govers, T. A. Quine, and G. Heckrath (2006), Modeling soil erosion induced carbonfluxes between soil and atmosphere onagricultural land using SPEROS-C, inSoil Erosion and Carbon Dynamics, edited by E. J. Roose et al., pp. 37–51, CRC Press, Boca Raton, Fla.

Virto, I., Gartzia-Bengoetxea, N., Fernández-Ugalde, O., 2011. Role of organic matter and carbonates in soil aggregation estimated using laser diffractometry. Pedosphere 21, 566–572.

Wang, Z., G. Govers, K. Van Oost, W. Clymans, A. Van den Putte, and R. Merckx. 2013. Soil organic carbon mobilization by interrill erosion: Insights from size fractions, J. Geophys. Res. Earth Surf., 118, 348–360.

Wang, Z., S. Doetterl, M. Vanclooster, B. van Wesemael, and K. Van Oost (2015), Constraining a coupled erosion and soil organic carbon modelusing hillslope-scale patterns of carbon stocks and pool composition,J. Geophys. Res. Biogeosci.,120, 452–465

Warrington, D.N., Mamedov, A.I., Bhardwaj, A.K., Levy, G.J., 2009. Primary particle size distribution of eroded material affected by degree of aggregate slaking and seal development. European J. Soil Sci. 60, 84 – 93.

Wright, A. F., Bailey, J. S., 2001. Organic carbon, total carbon, and total nitrogen determinations in soils of variable calcium carbonate contents using a Leco CN-2000 dry combustion analyzer. Commun. Soil Sci. Plant 32(19-20), 3243–3258.

Wu, H.B., Guo, Z.T., Gao, Q., Peng, C.H., 2009. Distribution of soil inorganic carbon storage and its changes due to agricultural land use activity in China. Agr. Ecosyst. Environ. 129 (4), 413–421.

Xiao, L., Hu, Y., Greenwood, P., and Kuhn, N. J. 2015. The use of a raindrop aggregate destruction device to evaluate sediment and soil organic carbon transport, Geogr. Helv., 70, 167–174.

Zamanian, K., Pustovoytov, K., Kuzyakov, Y., 2016. Pedogenic carbonates: Forms and formation processes. Earth-Science Reviews 157, 1–17.

Zhang, H., Liu, S., Yuan, W., Dong, W., Ye, A., Xie, X., Chen, Y., Liu, D., Cai, W., Mao, Y. 2014. Inclusion of soil carbon lateral movement alters terrestrial carbon budget in China. Sci Rep. 4, 7247.

Zheng H, Liu W, Zheng J, Luo Y, Li R, Wang H, Qi, H., 2018. Effect of long-term tillage on soil aggregates and aggregate-associated carbon in black soil of Northeast China. PLoS ONE 13(6), e0199523

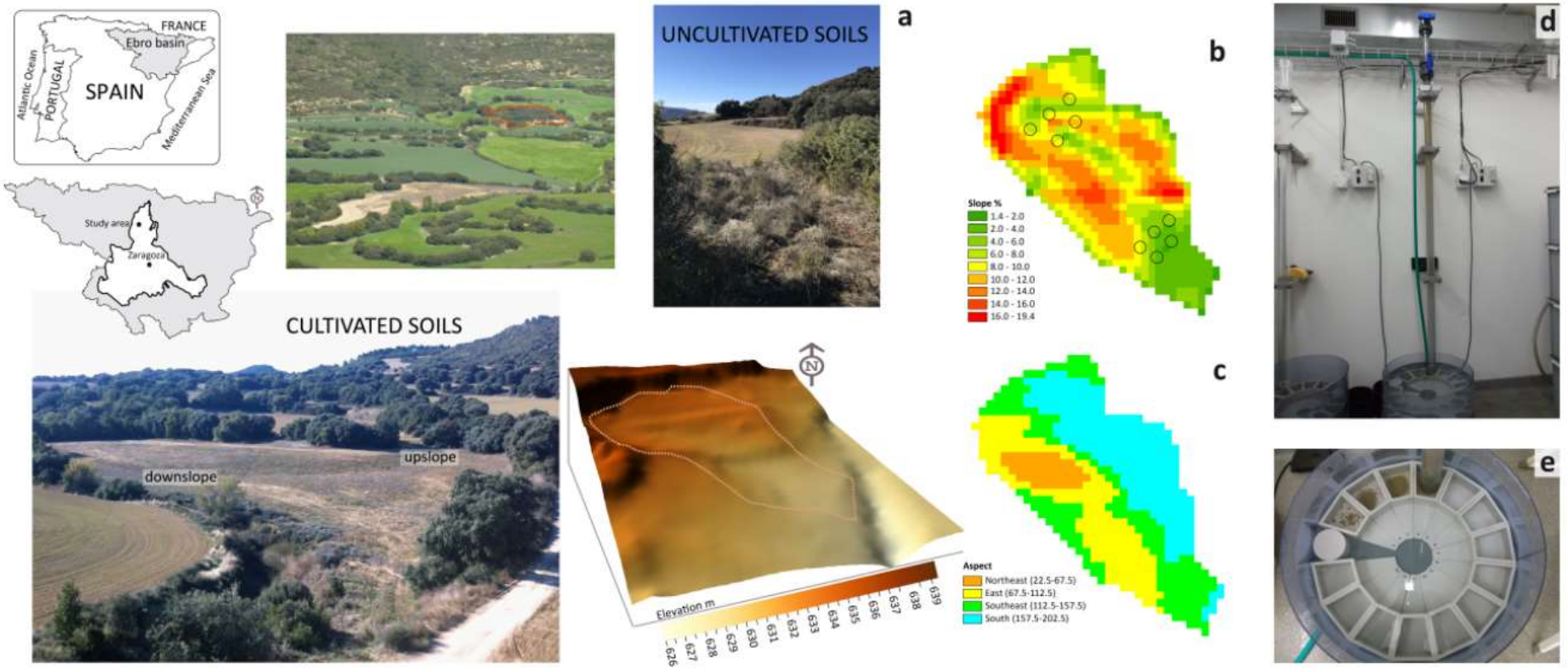

Fig. 1. a) Location of the study area in the central part of the Ebro basin (NE Spain) and 3Dview of the digital elevation model (2.5 m) of the hydrological unit and photographs of the hydrological unit and uncultivated and undisturbed soil under forest vegetation cover, b) slope map of the hydrological unit with the selected sampling points (circles) at the two established sampling areas at upslope and downslope positions, c) aspect map of the hydrological unit d) the settling tube apparatus, e) the turntable to collect the five settling samples.

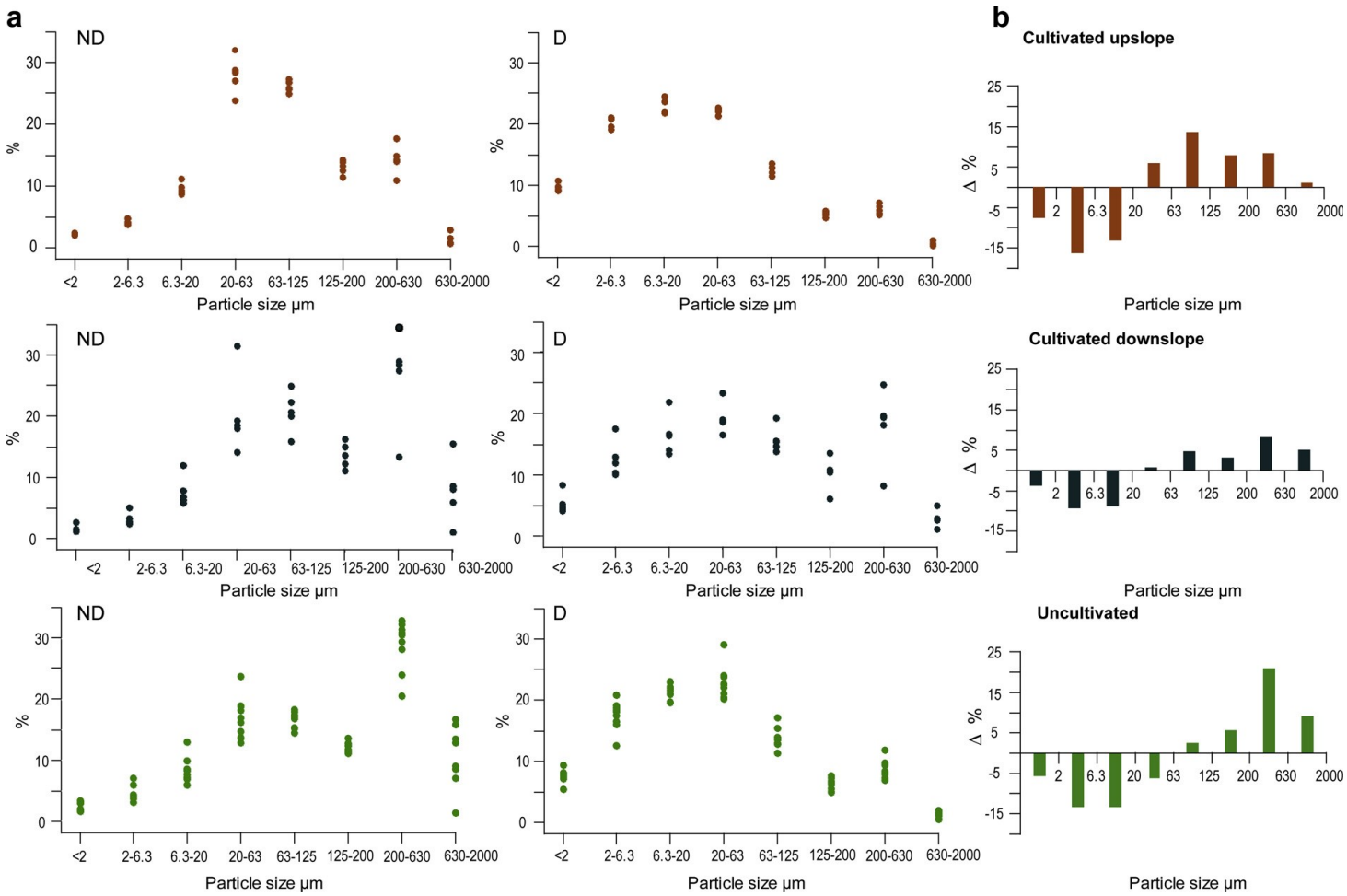

Fig. 2. a) Plots of the non-dispersed (ND) and dispersed (D) particle size distributions in cultivated upslope and downslope and uncultivated soil samples. b) Barplots of the difference between the values of the mean particle size content (%) in non-dispersed and dispersed study soils.

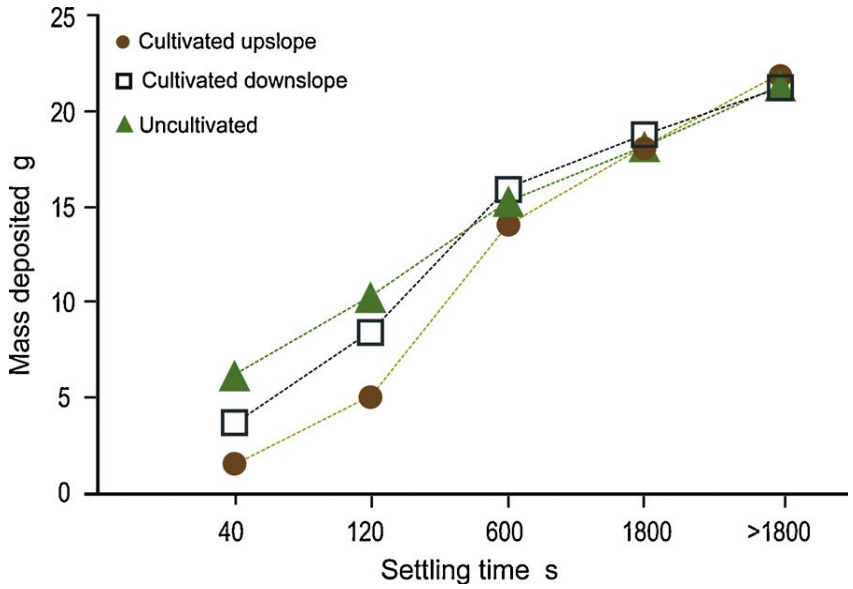

Fig. 3. Cumulative aggregate distribution curves of cultivated upslope and downslope and uncultivated soil.

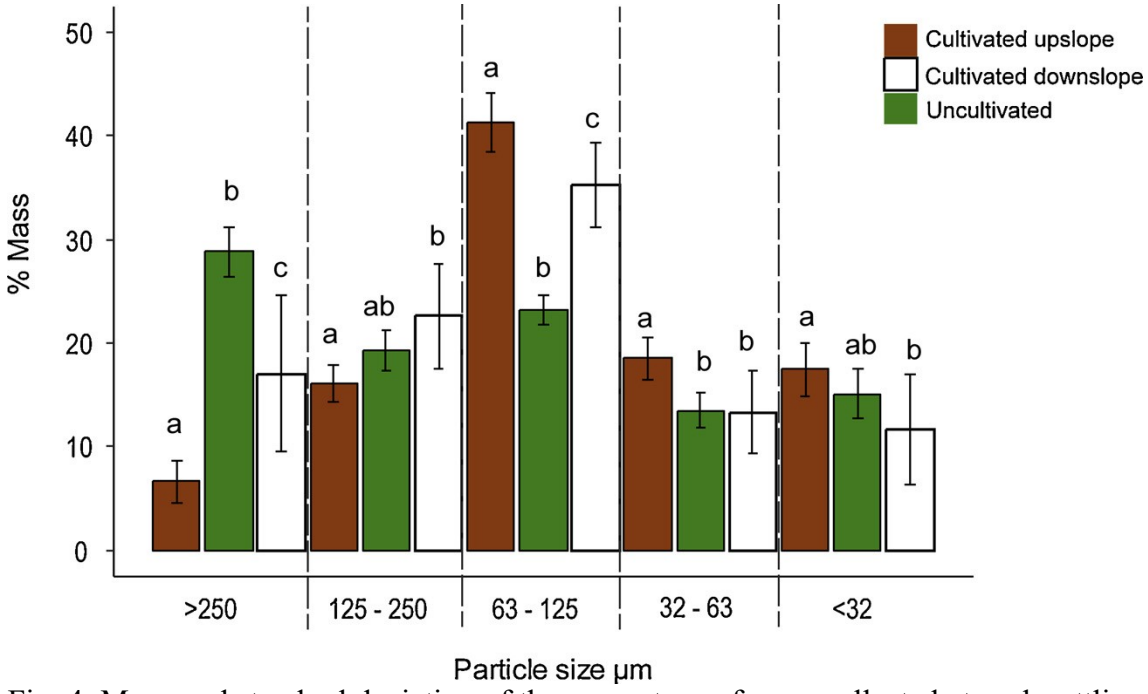

Fig. 4. Mean and standard deviation of the percentage of mass collected at each settling size classes in cultivated upslope and downslope and uncultivated soils.
Different letters indicate a significant difference ($p < 0.05$) between the mean values by comparing the three different groups of soil samples.

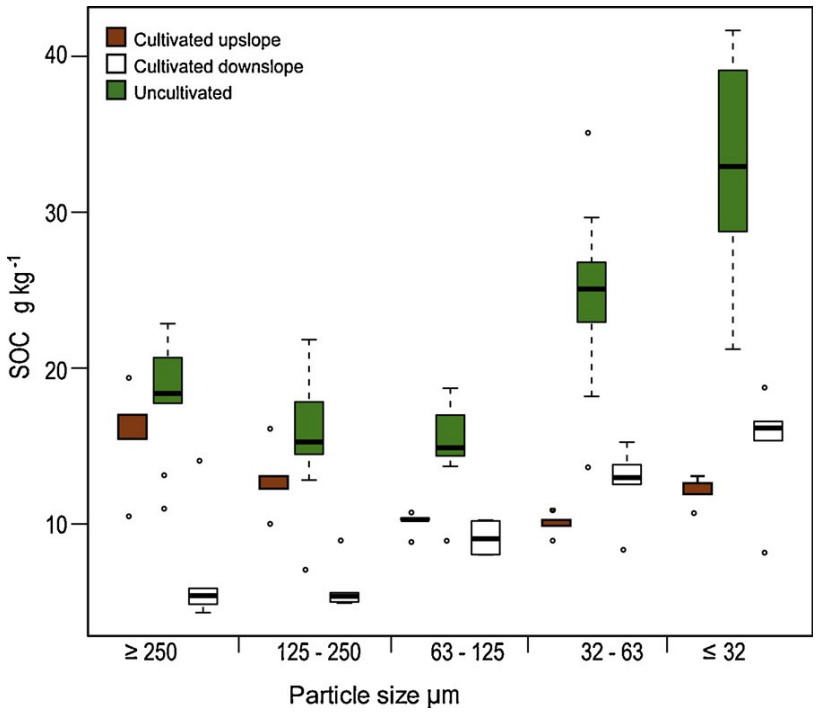

Fig. 5. Boxplots of SOC (g kg−1) at each of the settling size classes class in the cultivated upslope and downslope and uncultivated soil samples.

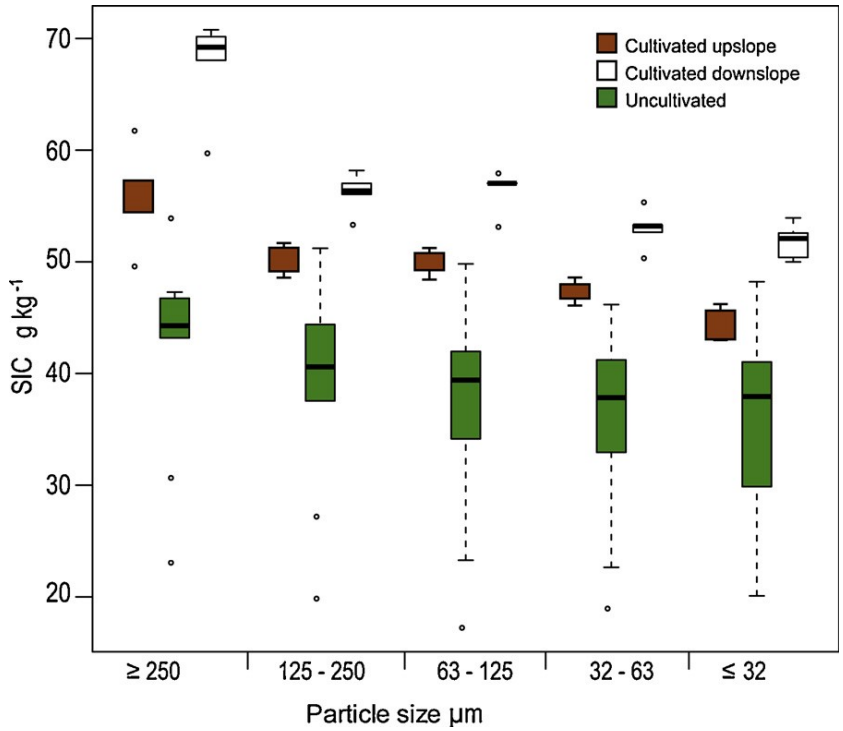

Fig. 6. Boxplots of SIC (g kg−1) at each of the settling size classes in the cultivated upslope and downslope and uncultivated soil samples.

Table 1 The five settling velocities based on equivalent quartz size classes (EQS).

EQS μm	Settling velocity m s^{-1}	Settling time s
>250	>$4.5x10^{-2}$	<40
250 - 125	$4.5x10^{-2}$ - $1.5x10^{-2}$	40 - 120
125 - 63	$1.5x10^{-2}$ - $3.0x10^{-3}$	120 - 600
63 - 32	$3.0x10^{-3}$ - $1.0x10^{-3}$	600 - 1800
<32	< $1.0x10^{-3}$	>1800

Table 2 Mean and standard deviation of the percentage of the eight established categories of particle sizes for non-dispersed (ND) and dispersed (D) soil samples under cultivation at upslope and downslope positions and uncultivated soils. Different letters within the same column indicate significant difference ($p<0.05$) by comparing the three different groups of soil samples and the two type of soil samples (ND and D).

		clay % <2	fine silt % 2-6.3	medium silt % 6.3-20	coarse silt % 20-63	very fine sand % 63-125	fine sand % 125-200	medium sand % 200-630	coarse sand % 630-2000
C - UPSLOPE	ND	2.2±0.2a	4.2±0.4a	9.7±1.0a	28.3±2.9a	26.4±0.9a	13.2±1.1a	14.5±2.4a	1.6±0.9a
	D	9.8±0.7b	20.4±0.9b	23.0±1.2b	22.3±0.5bc	12.6±0.8b	5.4±0.5b	6.1±0.8b	0.5±0.3a
C - DOWNSLOPE	ND	1.5±0.6a	3.1±1.1a	7.6±2.4a	20.0±6.5bcd	20.5±3.3c	13.4±2.1a	26.2±7.8c	7.7±5.1b
	D	5.4±1.7c	12.5±3.0c	16.4±3.3c	19.2±2.5cd	15.7±2.1d	10.2±2.7c	18.0±6.0d	2.5±1.6a
UNCULTIVATED	ND	2.1±0.6a	4.4±1.2a	8.2±2.0a	16.8±3.3d	16.3±1.4d	12.0±0.8a	29.7±4.4c	10.5±4.7b
	D	7.7±1.2d	17.7±2.2d	21.5±1.2b	23.0±2.5b	13.7±1.6b	6.3±0.9b	8.8±1.5b	1.3±0.4a

Table 3 Mean and standard deviation of the mass collected at each settling size classes for non pre-wetted (NP) and pre-wetted (P) soil samples. Different letters within the same column indicate significant difference ($p<0.05$) by comparing the three different groups of soil samples and the two type of soil samples (NP and P).

		>250 µm	250 - 125 µm	125 - 63 µm	63 - 32 µm	<32 µm
		g	g	g	g	g
Cultivated upslope	NP	1.76±0.54 a	3.29±0.50 a	8.67±0.59 a	4.30±0.35 a	3.98±0.48 a
	P	1.47±0.45 a	3.54±0.44 ab	9.06±0.73 a	4.06±0.40 a	3.83±0.49 a
Cultivated downslope	NP	3.90±1.54 b	4.64±0.93 c	7.14±0.92 b	2.99±0.78 b	2.44±1.22 b
	P	3.63±1.61 b	4.80±1.04 c	7.51±0.85 b	2.84±0.85 b	2.49±1.13 b
Uncultivated	NP	6.44±0.70 c	4.22±0.44 bc	5.20±0.30 c	3.08±0.43 b	3.39±0.47 a
	P	6.16±0.65 c	4.14±0.64 bc	4.98±0.60 c	2.88±0.42 b	3.21±0.46 ab

Table 4. Analysis of variance for soil organic carbon

Source	Type III Sum of squares
landscape position	473.48
particle size	124.39
landscape position * size	261.49
Error	262.46

Adjusted R Squared = 0.723

Table 5. Analysis of variance for soil inorganic carbon

Source	Type III Sum of squares	df	Mean square	F	Sig.
landscape position	1230.30	2	615.15	27.41	0.000
particle size	5300.40	4	1325.10	59.05	0.000
landscape position * size	4018.48	8	502.31	22.38	0.000
Error	262.46	85	3.09		

Adjusted R Squared = 0.804